2013

Coupled LBM-DEM Simulations of Gas Fluidised Beds

J. R. Third
ETH Zürich, Switzerland

C. R. Müller
ETH Zürich, Switzerland

COUPLED LBM-DEM SIMULATIONS OF GAS FLUIDISED BEDS

J. R. Third[a]* and C. R. Müller[a]
[a] ETH Zürich
Leonhardstrasse 27
Zürich, CH-8092
*T: +41 44 632 5296; E: jthird@ethz.ch

ABSTRACT
The coupled CFD-DEM technique, which combines a computational fluid dynamics (CFD) description of the fluid phase with a discrete element method (DEM) model of the particles, is one of the most widely used numerical techniques for modelling gas-fluidized beds. Since the spatial resolution of the fluid phase is low in CFD-DEM models, these models require a closure relationship to describe the interaction between the fluid and particulate phases. However, this closure relationship is the greatest source of error in CFD-DEM simulations because it does not account for local variation in the solids volume fraction or the relative motion between particles. The aim of this work was to examine the ability of the CFD-DEM technique accurately to model gas-fluidized beds. The predictions of a CFD-DEM model were compared with those of a coupled lattice Boltzmann method-discrete element method (LBM-DEM) technique, which does not require a closure relationship for the fluid-particle interactions. The two methods were found to give good agreement for the pressure drop through packed and fluidized beds. However, for superficial gas velocities above U_{mf}, different forms of particle motion were predicted by the two methods.

INTRODUCTION
Since its introduction by Tsuji *et al.* (1), the coupled computational fluid dynamics-discrete element method (CFD-DEM) technique has become one of the most widely used techniques for modelling gas-fluidized beds. In these simulations each particle is modelled as a distinct entity, whereas the fluid flow is modelled in a volume-averaged manner using a large cell size, typically 3 times the particle diameter. Due to the low spatial resolution of the fluid model, it is not possible to compute the fluid-particle interactions directly in these simulations with the result that these models require a closure relationship, often called the drag law. In recent years closure relationships have been developed for CFD-DEM simulations using the lattice Boltzmann method (LBM), *e.g.* Beetstra *et al.* (2). However, the drag law remains the greatest source of error in CFD-DEM methods since even the most sophisticated expressions describe only the average force experienced by a particle and make no allowance for particle rotation or relative motion between the particles.

SIMULATION METHOD

CFD-DEM Approach
The coupled CFD-DEM model employed here is based on the work of Tsuji *et al.* (1). This model combines a discrete element method model of the particulate phase, Cundall and Strack (3), with a volume-averaged description of the fluid

phase, Anderson and Jackson (4). A method based on the SIMPLE algorithm, Pantaka (5), is employed to solve the volume-averaged Navier-Stokes equations and the fluid domain is divided into cubic fluid cells with side length equal to three times the mean diameter of the particles. Due to the low spatial resolution of this method the interaction between the fluid and particulate phases cannot be obtained directly from the computed flow field and must be estimated from the volume-averaged flow field using a correlation. In this work the drag force correlation proposed by Beetstra *et al.* (2) is used to estimate the fluid-particle interaction. The fluid phase is modelled as Newtonian and incompressible. A uniform steady inflow boundary condition is imposed for the gas at the bottom of the bed and a constant pressure condition is imposed at the top of the freeboard. Full slip boundary conditions are imposed for the gas at the front, rear and sidewalls of the bed.

A soft-sphere DEM model was adopted for the particulate phase. This approach models contacts between colliding particles by allowing them to overlap by a small amount. The contact forces between the particles are then calculated based on this overlap, the relative velocity between the particles and the history of the contact. In the normal direction a damped linear spring is employed and attractive forces between particles are prevented such that the force in the normal direction, F_n, for a collision between particles *i* and *j* is given by:

$$F_n = \max\left(0, k_{n_{ij}}\delta_n - 2\eta_n\sqrt{m_{ij}k_{n_{ij}}v_n}\right)$$

Here η_n is the damping factor in the normal direction, δ_n is the particle overlap, k_n is the normal stiffness, v_n is the relative velocity in the normal direction and m_{ij} is the effective mass defined as $\frac{1}{m_{ij}}=\frac{1}{m_i}+\frac{1}{m_j}$. In the tangential direction static friction is modelled as a damped linear spring and the magnitude of the tangential force is limited by Coulomb's law such that

$$F_t = \min\left(\mu k_{n_{ij}}\delta_n, k_{t_{ij}}\delta_t - 2\eta_t\sqrt{m_{ij}k_{t_{ij}}v_t}\right)$$

Here μ is the coefficient of friction, η_t is the damping factor in the tangential direction, k_t is the tangential stiffness and v_t is the relative velocity of the two surfaces in contact. The tangential displacement, δ_t, is defined as $\int v_t dt$. Table 1 gives the parameter values used for the simulations reported here. DEM simulations of beds composed of identical spherical particles can suffer from unwanted effects due to the ability of the particles to pack into a perfect lattice. To prevent these “crystallization effects”, a particle size distribution given by

$$P(d) = \frac{2}{d^3}\frac{d_{max}^2 d_{min}^2}{d_{max}^2 - d_{min}^2}$$

was applied to the particles within the bed. The bounds on this distribution, d_{min} and d_{max}, are 95 % and 105 % of the nominal particle size.

LBM-DEM Approach

The coupled LBM-DEM simulations reported here were performed using the same DEM model for the particulate phase as was employed for the CFD-DEM model described above. To allow the direct numerical simulation of gas-fluidized beds, i.e. without closure relationships, the DEM was coupled to a lattice-Boltzmann model of the fluid phase. In this work the incompressible LBM model proposed by He and Luo (6) was used to model the fluid phase and the immersed boundary method proposed by Noble and Torczynski (7) was used to impose a no-slip fluid boundary condition on the surface of the particles. The D3Q19 lattice was used to discretize velocity space and the BGK relaxation model was applied for the collision term. Consequently, the evolution equation for the lattice-Boltzmann model used here can be expressed as:

$$f_i(\boldsymbol{x}+\boldsymbol{e}_i\delta_t, t+\delta_t) - f_i(\boldsymbol{x},t) = \frac{1}{\tau}\left[1-\sum_s \mathrm{B}(\varepsilon_s,\tau)\right]\left[f_i(\boldsymbol{x},t) - f_i^{(eq)}(\boldsymbol{x},t)\right] + \sum_s \mathrm{B}(\varepsilon_s,\tau)\,\Omega_i^s$$

Here f_i is the local density distribution function, τ is the relaxation constant of the BKG model and ε_s is the fraction of the fluid node that is occupied by particle s. $f_i^{(eq)}$ is the local density distribution under equilibrium conditions, which can be expressed as:

$$f_i^{(eq)}(\boldsymbol{x},t) = w_i\left\{\rho+\rho_0\left[3(\boldsymbol{e_i}.\boldsymbol{u}) + \frac{9}{2}(\boldsymbol{e_i}.\boldsymbol{u})^2 - \frac{3}{2}\boldsymbol{u^2}\right]\right\}$$

Where w_i are the weighting coefficients of the D3Q19 model. Ω_i^s is an additional collision term that accounts for the interaction with the solid obstacle and is defined as:

$$\Omega_i^s = f_{-i}(\boldsymbol{x},t) - f_i(\boldsymbol{x},t) + f_i^{(eq)}(\rho,\boldsymbol{U}_s) - f_{-i}^{(eq)}(\rho,\boldsymbol{u})$$

$\boldsymbol{U}_s$ is the velocity of the solid particle at $\boldsymbol{x}$ and $\mathrm{B}(\varepsilon_s,\tau)$ is a weighting function given by:

$$\mathrm{B}(\varepsilon_s,\tau) = \frac{\mathcal{E}_s(\tau-0.5)}{(1-\mathcal{E}_s)+(\tau-0.5)}$$

No-slip boundary conditions were modelled on the front, rear and sidewalls by employing the "bounce-back" boundary condition. The method proposed by Zho and He (8) was used to model open boundaries in the flow direction. At the base of the bed a constant, uniform velocity was imposed, whereas the top of the bed was modelled using a constant pressure boundary condition.

Table 1: Simulation parameters

Parameter	**Value**
Particle density (kg/m^3)	1000
Gas density (kg/m^3)	1.14
Gas viscosity (Pa s)	1.8×10^{-5}
Particle diameter (mm)	0.9
Bed width (mm)	28.8
Bed height (mm)	57.6
Transverse bed thickness (mm)	5.4
Static bed height (mm)	26.1
Particle normal stiffness (N/m)	1000
Particle tangential stiffness (N/m)	500
Coefficient of restitution (-)	0.9
Coefficient of friction (-)	0.1
Velocity of fluidizing gas (m/s)	0.3
Number of particles	6144

RESULTS

To validate the LBM-DEM code implemented here, the fluid-particle interaction force calculated using the LBM-DEM method was compared to that predicted by the CFD-DEM model, and to the Ergun equation:

$$\frac{\Delta P}{L} = \frac{150\mu_g(1-\mathcal{E})^2 U}{\varepsilon^3 {d_p}^2} + \frac{1.75(1-\mathcal{E})\rho U^2}{\varepsilon^3 d_p}$$

Figure 1 shows the pressure drop through the bed as a function of the superficial velocity of the fluidizing gas for a CFD-DEM simulation. In this simulation the superficial gas velocity was first increased from 0 to 0.45 m/s using a step size of 0.03 m/s and was then decreased back to 0 with the same step size. Figure 1 shows that, up to U = 0.27 m/s, the pressure drop through the bed increases as U is increased. Above this value of U the bed is fluidized and the pressure drop through it remains approximately constant. When U is decreased the pressure drop through the bed remains approximately constant until U = 0.21 m/s. Below this velocity the bed returns to an unfluidized state. This unusual behaviour can be explained by considering the average void fraction within the bed before and after fluidization. The initial static height of the bed was 26.1 mm, leading to an average void fraction of 0.42. Once the bed had been fluidized and de-fluidized, it had a static height of 24.5 mm, equivalent to an average void fraction of 0.385. The pressure drops predicted by the Ergun equation for these two void fractions are also shown in Figure 1. These data demonstrate excellent agreement between the CFD-DEM simulation and the Ergun equation when the bed is in an unfluidized state. Due to the high initial void fraction of the bed, a large superficial gas velocity is required to achieve a sufficient pressure drop through the bed to support the weight of the bed. Once the bed has been fluidised it is able to adopt a configuration with a lower void fraction, meaning that the weight of the bed can be supported at a lower superficial gas velocity. For the LBM-DEM simulations the total force acting on the particles due to the fluid was calculated. This force was divided by the cross-sectional area of the bed to give the pressure drop due to fluid-particle interactions and is plotted in Figure 1 for four values of U. The pressure drop predictions of the LBM-DEM simulations are slightly below the prediction of the CFD-DEM simulation for superficial gas velocities below the minimum fluidisation velocity. Despite this discrepancy, the agreement between the two methods is very good, which suggests that the implementation of the LBM-DEM model is correct.

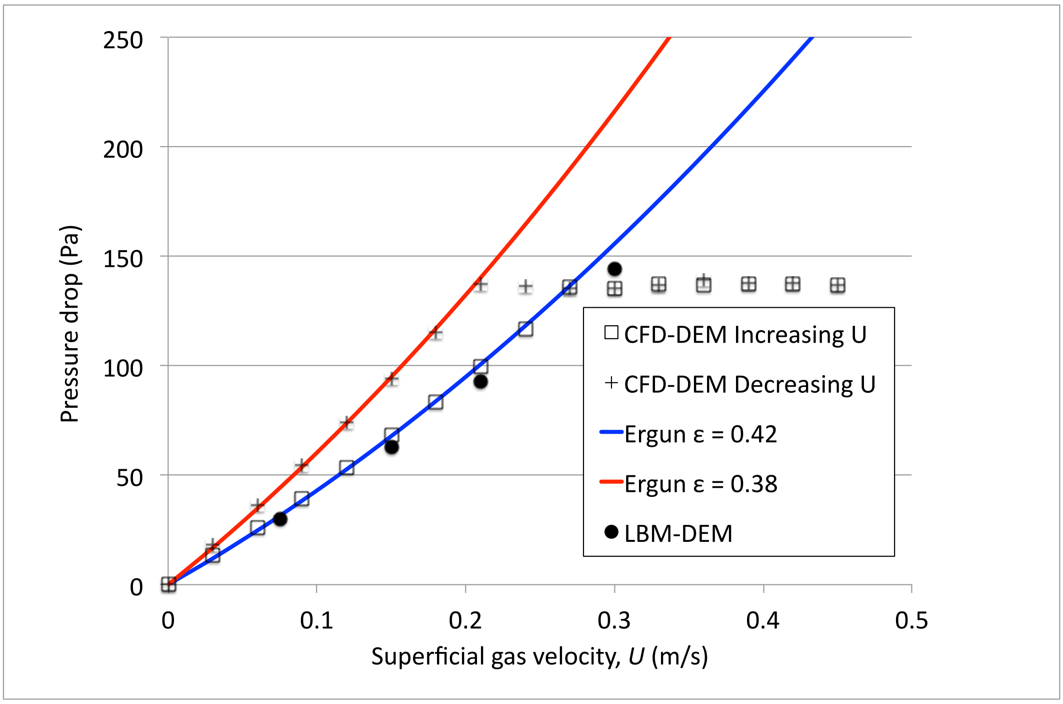

Figure 1: Pressure drop as a function of the imposed superficial gas velocity. Comparison of results from CFD-DEM and LBM-DEM simulations with the prediction of the Ergun equation.

Figure 2 shows the gas velocity in the vertical direction at the start of the simulation and after 1.25 s of simulated time for the LBM-DEM method. The gas velocities are plotted for a vertical plane located in the centre of the smallest dimension of the bed.

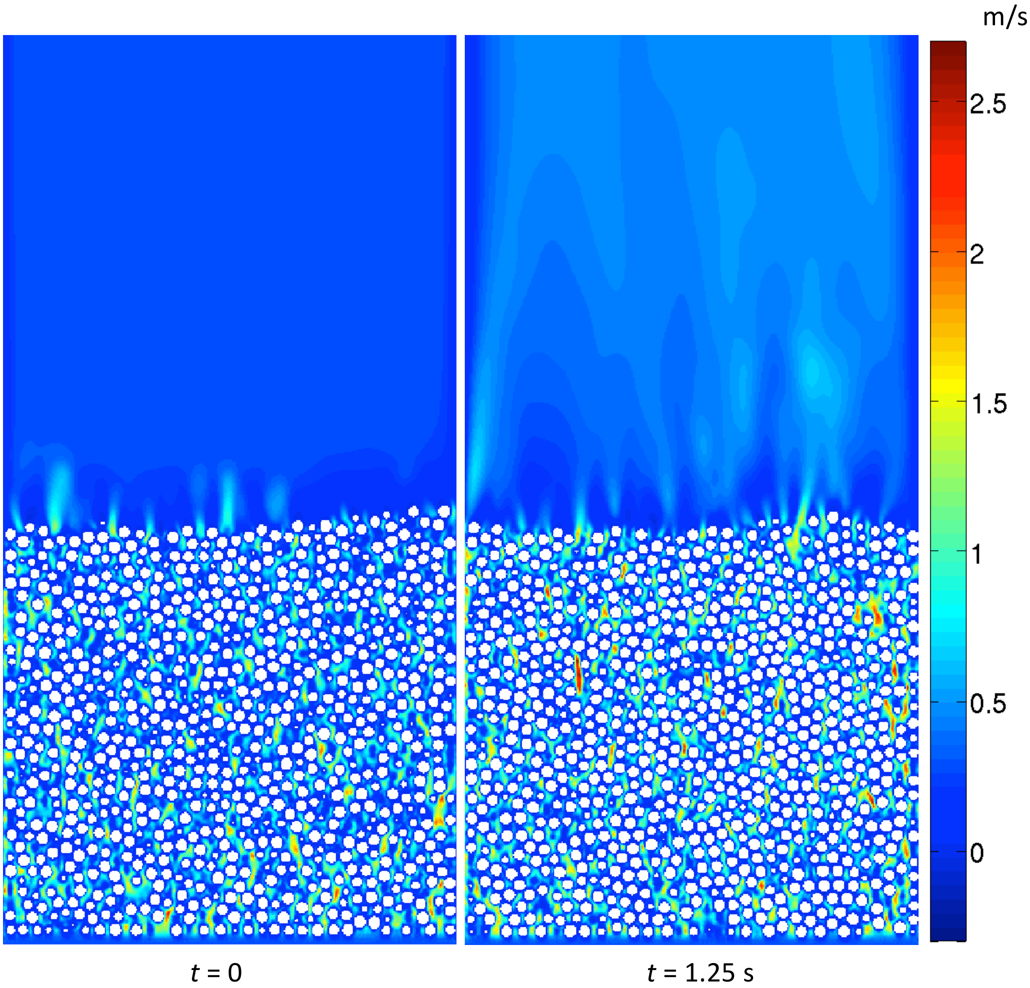

Figure 2: Gas velocities predicted by the LBM-DEM technique for a superficial gas velocity of 0.3 m/s.

Figure 3 shows snapshots of the particle positions after 1.25 s of simulated time for CFD-DEM and LBM-DEM simulations with a superficial gas velocity of 0.3 m/s. These images show a clear difference between the particle motion predicted by the two models. The CFD-DEM model predicts horizontal voids that rise through the bed. These voids span the full transverse thickness of the bed and dominate particle motion within the bed. In contrast, the LBM-DEM model does not predict voids that span the thickness of the bed. Instead, particles are observed to move upwards in the centre of the smallest dimension of the bed and flow downward at the front and rear walls. Further work is required to understand the cause of this discrepancy. One possibility may be that the different particle motion arises due to the way in which the boundary conditions are modelled in the two simulation methods. In the LBM-DEM model no-slip boundaries were imposed on the lateral walls of the bed, whereas full-slip boundaries were modelled in the CFD-DEM simulation due to the size of the fluid cell required by this method.

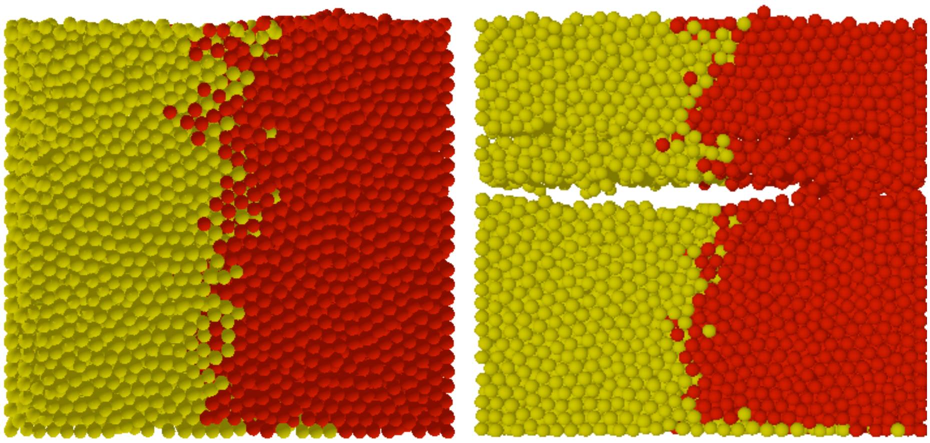

a) LBM-DEM b) CFD-DEM

Figure 3: Snapshots of the particle positions after 1.25 s for LBM-DEM and CFD-DEM simulations.

CONCLUSIONS

A method based on the LBM has been implemented to allow the direct numerical simulations of gas-fluidized beds. This method was validated by comparing predictions for the total force acting on a bed of particles with predictions from a CFD-DEM simulation of the same system and with the Ergun equation. The newly implemented method was found to give excellent agreement with both the CFD-DEM model and the Ergun equation. For superficial gas velocities above U_{mf}, different forms of particle motion were predicted by the two simulation methods. The CFD-DEM predicted voids that span the transverse thickness of the bed, whereas the LBM-DEM predicted a convection-like motion in which particles rise in the centre of the bed and fall close to the front and rear walls. Further work is required to establish the cause of this discrepancy.

NOTATION

d_p	particle diameter
dt	timestep of the numerical scheme
f_i	particle distribution function
F_n	contact force in the normal direction
F_t	contact force in the tangential direction
k_n	stiffness of the normal spring
k_t	stiffness of the tangential spring
m_i	mass of particle i
t	time
$\boldsymbol{u}$	velocity vector
U	superficial velocity of fluidising gas
U_{mf}	superficial velocity of fluidising gas at minimum fluidisation

U_s velocity of the solid phase
v_n relative velocity between particles in the normal direction
v_t relative velocity between particles in the tangential direction
w_i weighting coefficients of the LBM model
$\boldsymbol{x}$ position vector

Greek letters

δ_n overlap between contacting particles
δ_t tangential displacement of contact
ε void fraction of the bed
ε_s fraction of an LBM cell occupied by particles
η_n normal damping factor
η_t tangential damping factor
μ coefficient of friction
μ_g viscosity of the gas
ρ density of the gas
τ relaxation constant of the BKG model
Ω collisional term to account for interaction with the solid phase

REFERENCES

1. Y. Tsuji, T. Kawaguchi and T. Tanaka, Discrete particle simulation of 2-dimensional fluidized beds. *Powder Technol.*, 77(1): 79- 87, 1993.
2. R. Beetstra, M. A. van der Hoef and J. A. M. Kuipers, Drag force from lattice Boltzmann simulations of intermediate Reynolds number of past mono and bidisperse arrays of spheres. A.I.Ch.E. Journal 53(2): 489-501, 2007.
3. P. A. Cundall & O. D. L. Strack, A discrete numerical model for granular assemblies. Geotechnique, 29: 47-65, 1979.
4. T.B Anderson, R. Jackson, A fluid mechanical description of fluidized beds. Ind. Eng. Chem. Fund 6: 527-539, 1967.
5. S. V. Patanka, Numerical heat transfer and fluid flow. Taylor & Francis, 1980
6. X. He and L-S. Luo, Lattice Boltzmann Model for the Incompressible Navier-Stokes Equation. *J. Stat. Phys.*, 88: 927-944. 1997.
7. D. R. Noble and J. R. Torczynski, A Lattice-Boltzmann Method for Partially Saturated Computational Cells. Int. J. Mod. Phys. C, 9(8): 1189-1201, 1998.
8. Q. Zhou and X. He, On pressure and velocity boundary conditions for the lattice Boltzmann BGK model. Phys. Fluids, 9(6): 1591-1598, 1997